ACS Macro Letters

Letter

pubs.acs.org/macroletters

Fast Polymer Diffusion through Nanocomposites with Anisotropic Particles

Jihoon Choi,[†] Nigel Clarke,[‡] Karen I. Winey,[†] and Russell J. Composto[†,*]

[†]Department of Materials Science and Engineering, University of Pennsylvania, Philadelphia, Pennsylvania, United States

[‡]Department of Physics and Astronomy, University of Sheffield, Sheffield, S3 7RH, United Kingdom

Supporting Information

ABSTRACT: Polymer nanocomposites (PNCs) have characteristic length scales associated with both the nanoparticles (i.e., size and interparticle distance) and the polymer molecules (i.e., tube diameter of entanglement and radius of gyration; R_g). When the nanoparticle (NP) and polymer length scales are comparable, the polymer dynamics exhibit contrasting behavior for NPs differing only in size and shape. For spherical NPs and short anisotropic NPs, the polymer diffusion coefficient decreases monotonically with NP concentration. However, for long anisotropic NPs, polymer diffusion slows down at low NP concentration and recovers for NP concentrations above the critical concentration for network formation. By spanning intermediate ranges of nanoparticle size and shape, the role of the NP geometric parameters on the polymer dynamics is substantially advanced, thereby providing new routes toward controlling polymer dynamics and viscoelasticity of PNCs.

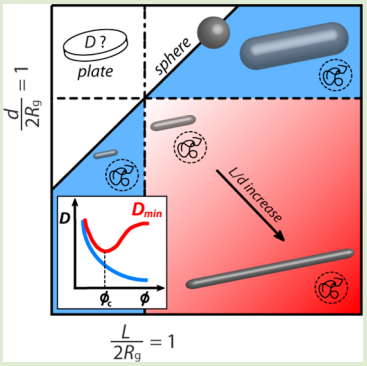

Novel functional materials can be invented and produced by judiciously combining existing materials, such as adding metallic nanoparticles to polymers to create flexible devices with tunable dielectric, optical, and electrical properties.[1−3] While polymer nanocomposites (PNCs) take advantage of the low cost and processability of polymers, nanoparticles (NPs) can both add orthogonal functionality and profoundly change the fundamental polymer dynamics and processability.[4,5] In particular, at high loadings, spherical and rod-like nanoparticles alter polymer dynamics in PNCs in significantly different ways. Spherical nanoparticles (silica) cause monotonic slowing down of the polymer diffusion, as generally expected.[6−8] In contrast, polymer diffusion through a matrix with thin-long nanoparticles (carbon nanotubes) initially decreases, reaches a minimum at a concentration at which the rods form a network, and then recovers as particle concentration increases.[9] These earlier reports involved different types of nanoparticles and a limited range of NP size and shape that prevented the reconciliation of these disparate behaviors in polymer dynamics. Here we use NPs with tunable rod like particle dimensions (diameter and length) to uncover the range of nanoparticle dimensions that distinguish these two behaviors and provide guidelines for new theories that capture the fast diffusion of macromolecules through a polymer network.

While the effects of NPs on mechanical, electrical, and thermal properties are well established,[1] a framework for understanding how NP shape and size impact polymer dynamics in PNCs is lacking. The dynamics of unentangled and entangled pure polymer melts are captured by Rouse and reptation models, respectively, theoretical models describing polymer dynamics in the presence of NPs require greater complexity, because PNCs involve NP−polymer and NP−NP interactions, size and shape of NPs, polymer size, polymer density, and entanglement density. During the past decade, local segmental dynamics near spherical NPs have been studied to understand how attractive and repulsive NP−polymer interactions influence PNC properties.[10−15] For instance, both experimental and theoretical studies have reported favorable polymer−surface interactions that allow for an immobilized polymer layer on NPs as well as a mobility gradient adjacent to NPs.[11−14] While these studies emphasize the effect of NP−polymer interactions and polymer packing on local dynamics and entanglements, the relaxation times that underlie processing, such as chain diffusion and viscosity, have not yet been described by the previously mentioned fundamental parameters in part because of lack of systematic studies.

In this letter we systematically identify the geometric parameters responsible for the recovery of fast polymer diffusion at high loadings. These experimental studies provide a comprehensive understanding that unifies the seemingly contradictory diffusive behavior in the presence of spherical and thin-long nanoparticles. This new insight will guide the rational combination of polymers and NPs to engineer materials with desired viscosity and processability. We employ nanorods for independent control of NP length and diameter to both smoothly change from a spherical to anisotropic NP shape and to vary NP size relative to the Gaussian polymer chains.

Received: June 9, 2014
Accepted: August 11, 2014
Published: August 22, 2014

   dx.doi.org/10.1021/mz500344h | ACS Macro Lett. 2014, 3, 886−891

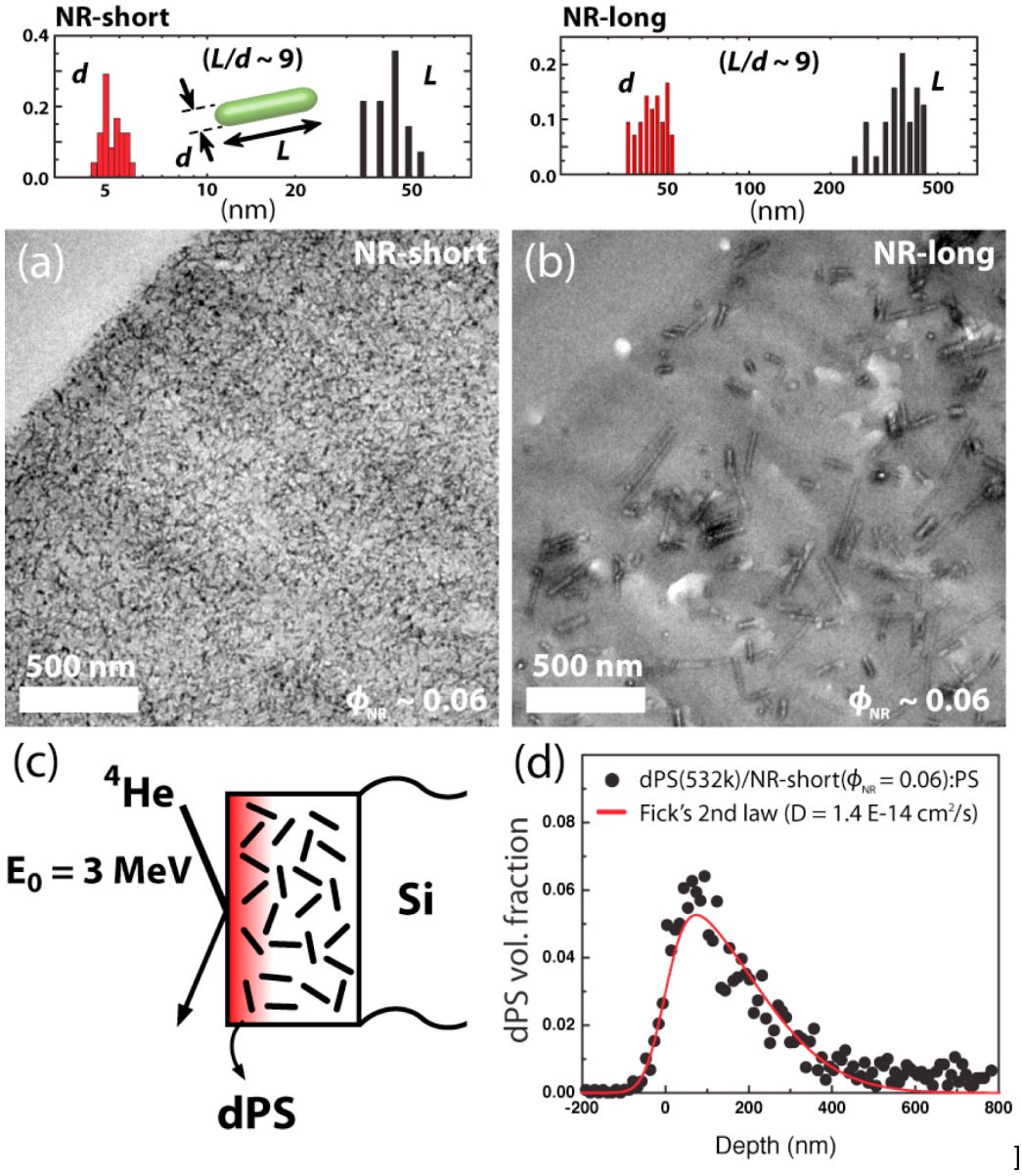

Figure 1. Transmission electron micrographs depicting morphology of (a) phenyl-capped TiO_2/PS nanocomposites ($\phi_{NR\text{-short}}$ = 0.06) and (b) phenyl-capped SiO_2-$[Ni(N_2H_4)_3]Cl_2$/PS nanocomposites ($\phi_{NR\text{-long}}$ = 0.06). Histograms show the distribution of diameter (d) and length (L) of nanorods, indicating a similar aspect ratio. (c) Elastic recoil detection (ERD) geometry with 3 MeV He^+ impinging on the bilayer and recoiling deuterium from dPS (red). (d) Representative volume fraction profile of dPS(532k) in TiO_2/PS ($\phi_{NR\text{-short}}$ = 0.06). Solid line is a fit of the depth profile using Fick's second law with $D = 1.40 \times 10^{-14}$ cm^2 s^{-1}.

Two phenyl-capped nanorods with similar aspect ratios (AR ~ 9) but different sizes, NR-short (TiO_2; L = 43.1 nm and d = 4.6 nm) and NR-long (SiO_2-$[Ni(N_2H_4)_3]Cl_2$; L = 371 nm and d = 43 nm) were prepared using standard Schlenk-line techniques.[16,17] For NR-short and NR-long, the surfaces are grafted with (chloromethyl)dimethyl phenylsilane that facilitate uniform dispersion of NRs in a polystyrene (PS; M_n = 650 kg/mol) matrix, as shown in the cross-sectional transmission electron micrographs (Figure 1a,b), respectively. These NRs are athermal in a PS matrix. To age the matrix, the film was preannealed at 150 °C for 3 days. No change in NR dispersion was observed, consistent with stable grafting. The glass transition temperatures (T_g) of the nanocomposites were 101 ± 1 °C, consistent with the prior results for PS mixed with phenyl-capped silica.[6] For diffusion studies, bilayers with a top deuterated polystyrene (dPS; M_n = 168−3400 kg mol^{-1}) with a thickness of 15 nm are deposited on a thick PNC (ϕ_{NR} = 0−0.1). Bilayers are annealed in a vacuum oven at T = 170 °C from a few hours to days. Tracer diffusion coefficients are determined by fitting the dPS volume fraction profiles determined by elastic recoil detection (ERD).[7,18] A representative dPS volume fraction (ϕ_{dPS}) profile is shown in Figure 1d, along with the best fit (solid line).

The tracer diffusion coefficients of entangled polymers (M_n = 168−3400 kg mol^{-1}) in PNCs containing NR-short and NR-long are shown in Supporting Information, Figures S1 and S2 as a function of NR volume fraction, ϕ_{NR}. Figure 2 shows dPS tracer diffusion coefficients in PNCs with NR-long normalized by that in pure polymer melts versus ϕ_{NR}. For the smallest tracers (168 and 532 kg mol^{-1}), normalized diffusion monotonically decreases as ϕ_{NR} increases, resulting in a nearly 50% reduction in D/D_0 for 10% NR-long or ϕ_{NR} = 0.1 (Figure

dx.doi.org/10.1021/mz500344h | ACS Macro Lett. 2014, 3, 886−891

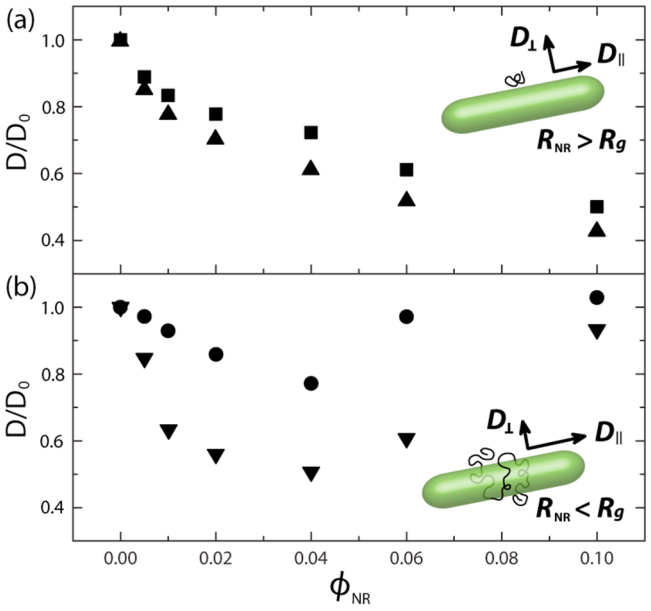

Figure 2. Reduced tracer diffusion coefficients of dPS for (a) M_n = 168 (squares) and 532 (triangles) kg mol^{-1} or (b) M_n = 1866 (circles) and 3400 (inverse triangles) kg mol^{-1} in nanocomposites containing NR-long (ϕ_{NR} = 0−0.1) exhibiting a monotonic decrease or a minimum of diffusion coefficients, respectively. Insets describe the local polymer diffusion in the direction parallel ($D_{||}$) and perpendicular ($D_{\perp}$) to NRs, depending on the relative size of the R_{NR} to R_g; (a) isotropic tracer diffusion ($D_{||} \cong D_{\perp}$) when $R_{NR} > R_g$ and (b) anisotropic tracer diffusion ($D_{||} > D_{\perp}$) when $R_{NR} < R_g$.

2a). In contrast, for the larger tracers (1866 and 3400 kg mol^{-1}), D/D_0 initially decreases, reaches a minimum near ϕ_{NR} = 0.04, and then recovers toward 1 as ϕ_{NR} approaches 0.1, namely, $D \sim D_0$ (Figure 2b). As shown schematically in the inset of Figure 2a, the NR-long radius (R_{NR}) is larger than the R_g of the smaller tracers, whereas for the larger tracers, $R_{NR} < R_g$ (inset, Figure 2b). For the latter case, the minimum diffusion coefficients (D_{min}) are observed near ϕ_{NR} = 0.04, which corresponds to the 3D percolation threshold (ϕ_p) for NR-long.[19]

At low NR loadings ($\phi_{NR} < \phi_p$), the diffusion coefficients of all four tracers decrease with increasing ϕ_{NR} independent of R_g/R_{NR}. For dilute NR loadings, NR-long are individually dispersed in the polymer matrix and act as impenetrable barriers that slow polymer diffusion, as proposed by several theories.[20−23] For example, Maxwell predicted a monotonic decrease of the diffusivity in a matrix of impenetrable discrete objects surrounded by a continuous phase that supports diffusion.[20] Because this model considers only the volume fraction of impenetrable objects, this model significantly underestimates the decrease in polymer diffusivity because it ignores entropic and enthalpic interactions, as well as perturbations in chain conformations due to the objects. An analytical study by Karatrantos et al. for PNCs with SWCNTs shows that an additional friction coefficient (f) between the SWCNT surface and monomers could account for the slowing down of tracer diffusivity for $\phi_{CNT} < \phi_p$.[23] In this model the fitting parameter is f/f_0 = 2500 (monomer−monomer friction coefficient, f_0 = 1.2 × 10^{-4} g s^{-1}, in bulk polystyrene melts), which is much greater than $N^{1/2}$ (N: degree of polymerization), indicating a high friction between PS monomers and SWCNT.[23] A recent analytical model by Meth et al. based on excluded volume around the nanoparticle is in good agreement with a reduction in diffusion at a low volume fraction of spherical NPs.[22] Whereas these models introduce friction and excluded volume attributable to NPs, they do not capture the importance of NP size, shape, and separation (ϕ_{NR}) underlyng the behavior of D/D_0 exhibited in Figure 2a,b.

In PNCs containing carbon nanotubes (CNTs), a diffusion minimum and recovery is observed when the tracer size, R_g, is greater than the CNT radius.[24] The decrease and recovery of D was attributed to anisotropic polymer diffusion for ϕ_{CNT} values above the percolation threshold, which is 0.4% for CNTs with an aspect ratio of ∼35.[9] The inset of Figure 2b represents the anisotropic diffusion as slow, perpendicular and fast, parallel to the nanoparticles, denoted as $D_{\perp}$ and $D_{||}$. Using small-angle neutron scattering the R_g of PS chains in PNCs of CNT/PS increases with ϕ_{CNT} when $R_{CNT} < R_g$, but slightly decreases for $R_{CNT} > R_g$.[25] In the classic reptation model, the polymer diffusion coefficient is given by the mean-squared center of mass displacement during the relaxation time (τ); $D_{rep} \sim \langle \Delta r_c^2 \rangle / \tau$, where $\Delta r_c \approx R_g$. If τ is unchanged by the CNTs,[9] the diffusion coefficient scales with the degree of polymerization according to $R_g \sim N^{\alpha}$ where α is 0.6 at high CNT concentrations. On the basis of these experimental and theoretical studies, we propose that the nonmonotonic diffusive behavior is attributable to competing contributions. Namely, at low ϕ_{NR}, diffusion slows down because of the thermodynamics of mixing (entropic barrier and enthalpic interactions), whereas above ϕ_p, diffusion recovers because of polymer chain swelling due to geometric constraints imposed by NRs.

In prior studies of high aspect ratio SWCNT and low aspect ratio MWCNT, a sole criterion for recovery of diffusion was that the radius of the CNT (or nanorod) had to be smaller than the tracer chain, namely $R_{CNT} < R_g$. Figure 2b shows that a slowing down and recovery is a general phenomenon in polymer tracer diffusion in PNCs containing anisotropic NRs that are much shorter than SWCNT. Compared to SWCNT/PS, D_{min} in long-NR/PS is observed at a ϕ_{NR} that is about 10× greater. In SWCNT/PS, the ϕ_{NR} at D_{min} is correlated with the rheological percolation threshold ($\phi_{p\text{-}rheo}$), suggesting that a percolating network is a physical requirement for non-monotonic diffusive behavior. For MWCNT, the rheological percolation threshold ($\phi_{p\text{-}rheo}$) is 0.016, in a good agreement with excluded volume theory in the slender rod limit (ϕ_p = 0.017 for L/d = 25.6).[19] Figure 2b shows that tracer diffusion in NR-long/PS reaches a minimum value, D_{min}, near ϕ_{NR} = 0.04, in excellent agreement with excluded volume theory (ϕ_p = 0.0424 for L/d = 8.6). Thus, the present studies demonstrate that network formation is a general criteria for observing a D_{min}.

Whereas the NR-long studies reinforce the criterion R_{NR}/R_g = 1, the effect of nanoparticle length (L) was not investigated because nanoparticles with requisite dimensions were not available. With advances in inorganic chemistry, anisotropic nanoparticles with L on the order of the polymer chain (i.e., R_g)[17,26] are now readily synthesized in reasonable quantities, allowing for systematic studies of polymer dynamics as a function of nanorod length. To complement studies in PNCs with short nanorods (L = 43.1 nm), denoted NR-short, were synthesized to explore tracer diffusion in a regime where rod length is smaller than tracer size, namely, $L < 2R_g$.

For PS matrices with NR-short, all dPS tracer chains are larger than the diameter of NR-short (d). Because the criterion $2R_g > d$ is satisfied, a minimum in diffusion, D_{min}, might be expected as the volume fraction of NR-short increases. As

dx.doi.org/10.1021/mz500344h | ACS Macro Lett. 2014, 3, 886−891

shown in Figure 3a, as ϕ_{NR} increases, the small dPS tracers (M_n = 168 and 532 kg mol^{-1}) exhibit an initial decrease in D/D_0 by

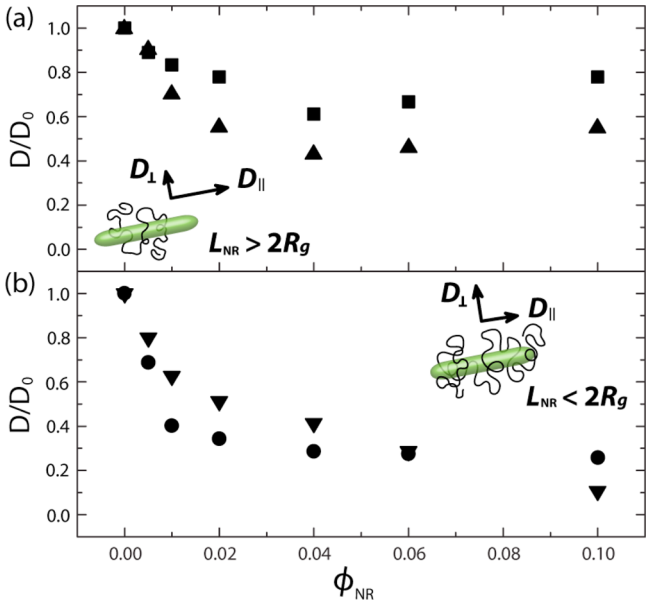

Figure 3. Reduced tracer diffusion coefficients of dPS for (a) M_n = 168 (squares) and 532 (triangles) kg mol^{-1} or (b) M_n = 1866 (circles) and 3400 (inverse triangles) kg mol^{-1} in nanocomposites containing TiO_2 (NR-short) nanorods ($\phi_{NR\text{-short}}$ = 0–0.1) exhibiting a minimum of diffusion coefficients or a monotonic decrease, respectively. Insets show (a) anisotropic and (b) isotropic tracer diffusion in the vicinity of nanorods when $2R_g$ of tracer molecules is smaller and larger than the length of the nanorods, respectively.

60 and 45%, respectively, and then a weak recovery to 80 and 60%, respectively, above ϕ_p. Although the recovery is weak, the nonmonotonic behavior of D/D_0 for these smaller dPS tracers (168 and 532 kg mol^{-1}) is similar to that observed in PNCs with NR-long (Figure 2b) and CNT.[9] For the larger dPS tracer chains (M_n = 1866 and 3400 kg mol^{-1}), where $2R_g > L$, Figure 3b shows that D/D_0 decreases monotonically as ϕ_{NR} increases, in contrast to the smaller dPS case. For dPS (1866 kg mol^{-1}), D/D_0 initially decreases strongly, by ~60% at $\phi_{NR} \sim 0.02$, and then more weakly as ϕ_{NR} approaches 0.10. For dPS (3400 kg mol^{-1}), whose size is twice the L of the NR-short (i.e., $2R_g > L$), D/D_0 decreases monotonically, similar to D/D_0 behavior in PNCs with spherical NPs. Thus, tracer diffusion in these PS/NR-short PNCs indicates that the degree of recovery depends on the ratio of NR length to chain size or $L/2R_g$. This new result shows that polymer diffusion in PNCs depends not only on NP shape (e.g., sphere vs rod), but also on the characteristic NP dimensions (d and L) relative to the tracer size, $2R_g$. For smaller tracer chains ($L/2R_g \gg 1$), nonmonotonic behavior of D is attributed to anisotropic diffusion (Figure 3a, inset). However, when the tracer size is larger than the NR length ($L/2R_g < 1$), only monotonic slowing down is observed similar to isotropic (spherical) nanoparticles, indicating that shape anisotropy is unable to create anisotropic polymer diffusion for $\phi_{NR} > \phi_p$.

By plotting tracer diffusion coefficients versus tracer molecular weight (M_n) at fixed ϕ_{NR}, the scaling behavior $D \sim M^{\nu}$ can be evaluated to provide insight into the effect of nanorods on polymer dynamics. Polymer dynamics in entangled polymer melts is described by reptation, $D \sim M^{-2}$.[27] Because NRs can influence local segmental dynamics[10−15] as well as topological constraints,[25] the scaling relation in the presence of particles likely differs from the reptation model and varies with ϕ_{NR}. At low NR loadings ($\phi_{NR} < \phi_{min}$ = 0.04), polymer diffusion may obey reptation if chain conformation and local friction are unperturbed by NRs. At fixed, low NR concentration (ϕ_{NR} = 0.04) Figure 4a shows that

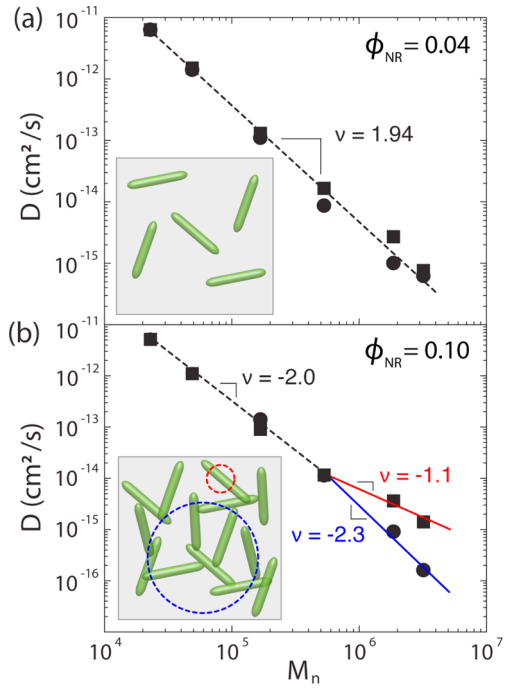

Figure 4. Dependence of tracer diffusion coefficients on the molecular weights in the nanocomposites containing NR-long (squares) or NR-short (circles) for (a) ϕ_{NR} = 0.04 and (b) ϕ_{NR} = 0.10, respectively. (a) The tracer diffusion coefficient in the nanocomposites (ϕ_{NR} = 0.04) follows the scaling relation $D \sim M^{-1.94}$, in agreement with the Doi–Edwards model of chain reptation.[27] (b) Divergent scaling behaviors for NR-long ($D \sim M^{-1.1}$) and NR-short ($D \sim M^{-2.3}$) are observed at higher tracer molecular weights (M_n > 500 kg mol^{-1}). Red and blue dashed circles show the corresponding relative size between nanorods and tracer polymer chains for NR-long and NR-short, respectively. The error bars are less than the symbol size in all cases.

the tracer diffusion coefficient of dPS into matrices with NR-long and NR-short scales as M^{-2} in agreement with the reptation mechanism. However, for higher NR concentrations ($\phi_{NR} > \phi_{min}$), the friction of monomers in contact with the NR can dominate the overall friction coefficient $F \sim fN(\phi_{NR})^m$, where the number of monomer-surface contacts per chain, $N(\phi_{NR})$, depends on surface geometry (e.g., m = 0.5 and <0.5 for flat and curved surfaces, respectively).[23,28] For an entangled melt near an attractive flat surface, the characteristic time to escape the confining tube of length l is $\tau \sim M^{2.5}$.[28] Because τ is proportional to l^2/D_{tube}, where $l \sim M$ and $D_{tube} \sim kT/F$ scales as $M^{-0.5}$, the diffusion coefficient $D_{rep} \sim \langle \Delta r_c^2 \rangle / \tau$ is predicted to scale as $M^{-1.5}$. For SWCNT/PS, where $R_{SWCNT} < R_g$, Tung et al. showed that R_g is larger than an unperturbed Gaussian chain[25] and described by $R_g \sim aN^{\alpha}$, where $\alpha > 0.5$. The PS/NR-long PNCs at high tracer molecular weight ($2R_g > d$ and $2R_g < L$) exhibit an experimental scaling relation of $D \sim M^{-1.1}$; see red line in Figure 4b. This finding is attributed to two contributions, namely, monomer-NR friction and expanded

dx.doi.org/10.1021/mz500344h | ACS Macro Lett. 2014, 3, 886–891

chain conformation, and provides new insight into the mechanism underlying the recovery of D/D_0 above ϕ_{min}.

In contrast to NR-long, dPS diffusion in the presence of NR-short at high loadings ($\phi_{NR} = 0.10 > \phi_{min}$, Figure 4b) scales as $\nu = -2$ and -2.3 for M less than and greater than ~500 kg/mol, consistent with dPS diffusion in the presence of isotropic NPs (Figure S3). For NR-short with $L/2R_g < \sim 1$, tracer diffusion is not affected by NP geometry and diffusion occurs similarly to the isotropic case, as indicated in the inset of Figure 4b (blue dashed line). The stronger dependence of tracer diffusion on M, namely, $D \sim M^{-2.3}$, may result from the entropic barriers associated with strong confinement as well as the similar size of polymer chains to the network formed by percolated NR-short.

From tracer diffusion in the presence of spherical silica and CNTs as well as the new nanorod studies presented in this letter, the geometric criterion that distinguishes monotonic and nonmonotonic diffusive behavior can be identified for the first time. Nonmonotonic behavior requires (1) the nanorod diameter must be less than the tracer size ($d < 2R_g$) and (2) the nanorod length must be greater than the tracer size ($L > 2R_g$), namely, $d < 2R_g < L$. Note, the criterion for nonmonotonic behavior of polymer diffusion is insensitive to the diameter and length distributions of nanorods in this study (Tables S1 and S2). By plotting particle diameter and length relative to tracer size, Figure 5 consolidates all diffusion studies into either monotonic or nonmonotonic (red region) behavior. This plot quantitatively captures experimental tracer diffusion results in PNCs containing nanoscale particles having a wide range of shape anisotropy ($1 \leq L/d < \sim 35$). For comparison, monotonic slowing down in the presence of isotropic (spherical) NPs (stars) that are both larger and smaller than

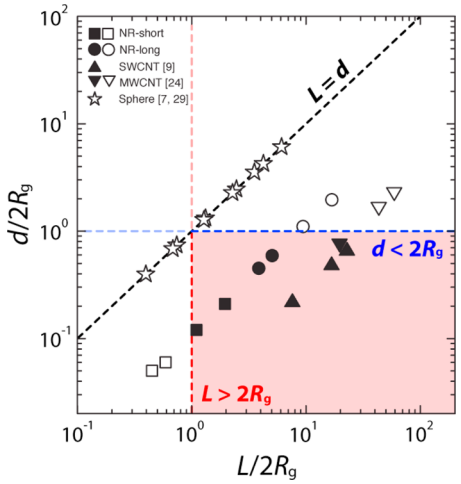

Figure 5. Threshold parameters (i.e., normalized diameter and length) for the onset of the minimum of tracer diffusion coefficient in nanocomposites depending on the dimensionality of the nanoparticle, that is, zero-dimensional (0D; sphere) and one-dimensional (1D; rod). Circles and squares represent NR-long (see Figure 2) and NR-short (see Figure 3), respectively. Data from the literature on single wall carbon nanotube (SWCNT), multiwall carbon nanotube (MWCNT), and nanosphere are shown as triangles, inverse triangles, and stars, respectively. Closed symbols indicate the systems that exhibit a minimum tracer diffusion coefficient with increasing nanoparticle concentration, while open symbols correspond to systems without a minimum. Black, blue, and red dashed lines represent $L = d$, $d = 2R_g$, and $L = 2R_g$, respectively. Red rectangle indicates the theoretical criterion for nonmonotonic diffusive behaviors.

$2R_g$ are shown across the diagonal where $L = d$. Note that tracer diffusion in the presence of SWCNTs which are thin and long is always nonmonotonic, whereas NR-long (and MWCNT) and NR-short display both behaviors depending on $d/2R_g$ and $L/2R_g$, respectively. This map indicates that both the diameter (d) and length (l) of the nanoparticles determine the mechanism of polymer diffusion in the presence of NPs at concentrations above the percolation of NRs. Thus, these studies provide valuable insights into tracer diffusion in polymer nanocomposites and motivate new models that incorporate the monomer-NP friction, chain expansion and nanoparticle size (d and L) relative to probe size $2R_g$.

■ ASSOCIATED CONTENT

Supporting Information

Full data of tracer diffusion in PNCs containing NR-short, NR-long, or spherical NPs. This material is available free of charge via the Internet at http://pubs.acs.org.

■ AUTHOR INFORMATION

Corresponding Author

*E-mail: composto@seas.upenn.edu.

Notes

The authors declare no competing financial interest.

■ ACKNOWLEDGMENTS

This research was primarily supported by the National Science Foundation NSF/EPSRC Materials World Network DMR-1210379 (R.J.C., K.I.W.), the EPSRC EP/5065373/1 (N.C.), and Dupont Central Research and Development (R.J.C.). Support was also provided by the NSF/MRSEC-DMR 11-20901 (K.I.W., R.J.C.) and Polymer Programs DMR09-07493 (R.J.C.). The authors thank Dr. Thomas R. Gordon and Prof. Christopher B. Murray for providing TiO_2 nanorods.

■ REFERENCES

(1) Winey, K. I.; Vaia, R. A. *MRS Bull.* **2007**, *32*, 314−319.
(2) Balazs, A. C.; Emrick, T.; Russell, T. P. *Science* **2006**, *314*, 1107−1110.
(3) Bockstaller, M. R.; Thomas, E. L. *J. Phys. Chem. B* **2003**, *107*, 10017−10024.
(4) Schneider, G. J.; Nusser, K.; Wilner, L.; Falus, P.; Richter, D. *Macromolecules* **2011**, *44*, 5857−5860.
(5) Kalathi, J. T.; Grest, G. S.; Kumar, S. K. *Phys. Rev. Lett.* **2012**, *109*, 198301.
(6) Gam, S.; Meth, J. S.; Zane, S. G.; Chi, C.; Wood, B. A.; Seitz, M. E.; Winey, K. I.; Clarke, N.; Composto, R. J. *Macromolecules* **2011**, *44*, 3494−3501.
(7) Choi, J.; Hore, M. J. A.; Meth, J. S.; Clarke, N.; Winey, K. I.; Composto, R. J. *ACS Macro Lett.* **2013**, *2*, 485−490.
(8) Lin, C.-C.; Gam, S.; Meth, J. S.; Clarke, N.; Winey, K. I.; Composto, R. J. *Macromolecules* **2013**, *46*, 4502−4509.
(9) Mu, M.; Clarke, N.; Composto, R. J.; Winey, K. I. *Macromolecules* **2009**, *42*, 7091−7097.
(10) Desai, T.; Keblinski, P.; Kumar, S. K. *J. Chem. Phys.* **2005**, *122*, 134910.
(11) Harton, S. E.; Kumar, S. K.; Yang, H.; Koga, T.; Hicks, K.; Lee, H.; Mijovic, J.; Liu, M.; Vallery, R. S.; Gidley, D. W. *Macromolecules* **2010**, *43*, 3415−3421.
(12) Liu, J.; Cao, D.; Zhang, L.; Wang, W. *Macromolecules* **2009**, *42*, 2831−2842.
(13) Starr, F. W.; Schrøder, T. B.; Glotzer, S. C. *Macromolecules* **2002**, *35*, 4481−4492.
(14) Montes, H.; Lequeux, F.; Berriot, J. *Macromolecules* **2003**, *36*, 8107−8118.

(15) Bogoslovov, R. B.; Roland, C. M.; Ellis, A. R.; Randall, A. M.; Robertson, C. G. *Macromolecules* **2008**, *41*, 1289−1296.
(16) Gao, C.; Zhang, Q.; Lu, Z.; Yin, Y. *J. Am. Chem. Soc.* **2011**, *133*, 19706−19709.
(17) Gordon, T. R.; Cargnello, M.; Paik, T.; Mangolini, F.; Weber, R. T.; Fornasiero, P.; Murray, C. B. *J. Am. Chem. Soc.* **2012**, *134*, 6751−6761.
(18) Composto, R. J.; Walters, R. M.; Genzer, J. *Mater. Sci. Eng. R* **2002**, *38*, 107−180.
(19) Mutiso, R. M.; Sherrott, M. C.; Li, J.; Winey, K. I. *Phys. Rev. B* **2012**, *86*, 214306.
(20) Maxwell, J. C.; Thomson, J. J. *A Treatise on Electricity and Magnetism*, Unabridged 3rd ed.; Dover Publications: New York, 1954.
(21) Crank, J. *The Mathematics of Diffusion*, 2nd ed.; Clarendon Press: Oxford, 1975.
(22) Meth, J. S.; Gam, S.; Choi, J.; Lin, C.-C.; Composto, R. J.; Winey, K. I. *J. Phys. Chem. B* **2013**, *117*, 15675−15683.
(23) Karatrantos, A.; Clarke, N. *Soft Matter* **2011**, *7*, 7334−7341.
(24) Mu, M.; Composto, R. J.; Clarke, N.; Winey, K. I. *Macromolecules* **2009**, *42*, 8365−8369.
(25) Tung, W.-S.; Bird, V.; Composto, R. J.; Clarke, N.; Winey, K. I. *Macromolecules* **2013**, *46*, 5345−5354.
(26) Thorkelsson, K.; Mastroianni, A. J.; Ercius, P.; Xu, T. *Nano Lett.* **2012**, *12*, 498−504.
(27) Doi, M.; Edwards, S. F. *J. Chem. Soc., Faraday Trans.* **1978**, *74*, 1789−1801.
(28) Zheng, X.; Sauer, B. B.; Van Alsten, J. G.; Schwarz, S. A.; Rafailovich, M. H.; Sokolov, J.; Rubinstein, M. *Phys. Rev. Lett.* **1995**, *74*, 407−410.
(29) Choi, J.; Hore, M. J. A.; Clarke, N.; Winey, K. I.; Composto, R. J. *Macromolecules* **2014**, *47*, 2404−2410.